Relativistic effects in the study of structure and electronic properties of UO_2 within DFT+U method

Mahmoud Payami and Samira Sheykhi
School of Physics and Accelerators, Nuclear Science and Technology Research Institute, AEOI, P.O. Box 14395-836, Tehran, Iran

E-mail: Mpayami@aeoi.org.ir

Abstract
Electrons of orbitals near to nuclei of heavy atoms acquire speeds comparable to the speed of light in vacuum. Therefore, to study the properties of crystals containing heavy atoms, it is necessary to take into account the relativistic effects. In this work, using the first-principles DFT+U method, we have calculated the electronic structure and geometric properties of uranium dioxide UO_2 within full-relativistic, scalar-relativistic, and non-relativistic formulations, and compared the results. It is shown that: (i) the non-relativistic scheme gives results very far form experimental values for both lattice constant and bang gap; (ii) in full-relativistic case which the spin-orbit effects are included, the Kohn-Sham band-gap is increased by 6.2% and the lattice constant decreases by 0.05% compared to scalar-relativistic one. Therefore, in the study of geometric properties of UO_2, using the scalar-relativistic regime is quite accurate and one does not need to perform much more expensive full-relativistic calculations whenever one does not study the electronic excitation properties.

Keywords: Uranium dioxide, Anti-ferromagnetism, Density-Functional Theory, Spin-orbit effect, Mott Insulator, DFT+U

1. Introduction

UO_2 is one of the common fuels used in nuclear power reactors. The experimental studies show that UO_2 has an anti-ferromagnetic (AFM) crystal structure with a 3k-order at temperatures less than 30 K, while at higher temperatures it assumes a para-magnetic form [1,2]. Analysis of earlier experimental results [3] had shown that the uranium and oxygen atoms occupied respectively the octahedral (4a) and tetrahedral (8c) symmetry positions of cubic space group $Fm\bar{3}m$ (No. 225) with lattice constant of 5.47 Angstrom, which is shown in Fig. 1. However, more recent XRD experiments [4] has shown that UO_2 crystallizes with a less symmetric cubic space group $Pa\bar{3}$ (No. 205) with oxygen atoms slightly displaced inside the cube.

The electronic structure of UO_2 has already been investigated by other researchers [5-14]. It is well-known that the ordinary approximations used in density-functional theory (DFT) [15, 16] description of the system usually lead to incorrect metallic behavior while it is experimentally found to be an insulator, the so-called "Mott insulator". The incorrect metallic prediction arises from the usual approximations in which the partially-filled "localized" *5f* and/or *6d* valence electrons in uranium atoms or *2p* valence electrons in oxygen atoms are treated by the same footing as other "delocalized" ones. To overcome this problem, one of the ways researchers commonly resort to, is the method of DFT+U [11, 17-19] which is computationally less expensive and also adopted here in our calculations; another method is using orbital-dependent hybrid functionals for the exchange-correlation (XC) energy functional [13].

It is well-known that electrons of orbitals near to nuclei of heavy atoms, here the uranium ones, acquire very high speeds comparable to the speed of light and therefore one has to take into account the relativistic effects. Some researchers have already investigated the relativistic effects of U-atom on the properties of UO_2 crystal using the LCAO method and obtained incorrect stable ferromagnetic phase with incorrect metallic properties for both relativistic and non-relativistic schemes [20]. To estimate the speed of inner electrons for U-atom, we use the simple Bohr model for hydrogen and ignore the electron-electron interactions. The speed of electron is given by $v_e = \sqrt{kZe^2 / m_e r}$ in which $k = 8.99\times10^9$, $m_e = 9.11\times10^{-31}$ and $e = 1.6\times10^{-19}$ in SI units. For U-atom, we take $Z = 92$, and using the positions of the peak of atomic wave-functions as the radii of Bohr orbits, we estimate the speeds of *1s*, *2p*, *3d*, and *4f* electrons. The results are tabulated in Table 1.

Table 1: Estimation of the speed for inner electrons of U and O atoms using the simple Bohr model. Here, a_0 =0.529 Angstrom and c is the speed of light $c \approx 3\times10^8\ m/s$.

atom	Z	nl	r_e/a_0	v_e/c
U	92	$1s$	0.008	0.80
		$2p$	0.041	0.40
		$3d$	0.114	0.20
		$4f$	0.286	0.10
O	8	$1s$	0.129	0.06

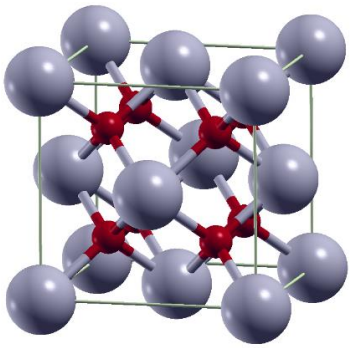

Fig. 1: UO_2 crystal structure at low temperatures with cubic space group $Fm\bar{3}m$ (No. 225) with lattice constant of 5.47 Angstrom. Grey and red balls represent uranium and oxygen atoms respectively.

The results in Table 1 show that for O atoms we do not need to take relativistic effects into account. However, for U atoms the speeds of inner electrons are comparable to that of light.

The relativistic effects are usually considered within two "scalar-relativistic" (spin-orbit interaction is negligible) and "full-relativistic" (spin-orbit effect is significant) levels. In the full-relativistic approach, one solves the Dirac-Kohn-Sham equations.

In this work, using the first-principles DFT+U method, we have calculated the electronic structure and geometric properties of uranium dioxide within full-relativistic (FR), scalar-relativistic (SR), and non-relativistic (NR) formulations, and compared the results. In all our calculations, the simplified model of 1k-order AFM configuration for uranium atoms were used. Also, for the geometry optimizations we have applied the constraint of $Fm\bar{3}m$ space group which does not affect much the results. Our calculations show that the equilibrium lattice constants in the FR and SR approaches differ slightly (by 0.05%) while the electronic gaps differ significantly (by 6.2%). On the other hand, the equilibrium lattice constants in the SR and NR cases differ relatively significantly (by 2%) and the difference in the energy gap is very large (64%). Therefore, in the study of UO_2, using the SR regime is quite accurate whenever one does not study the electronic excitation properties.

The organization of this paper is as follows. In Section 2 the computational details are presented; in Section 3 the calculated results are presented and discussed; Section 4 concludes this work.

2. Computational details

2.1 Pseudopotentials

For the atoms U and O, we have employed norm-conserving pseudo-potentials (NCPP) generated by the *APE* code [21]. To make the NCPP's transferable, we have applied nonlinear core correction in the generation step for all three NR, SR, and FR cases. For the NCPP generation in NR, SR, and FR cases, we have used the reference valence configurations of U(*6s2, 6p6, 7s2, 7p0, 6d1, 5f3*) and O(*2s2, 2p4*). In the FR case, the pseudo-potentials were generated by solving the Dirac's equation (Appendix A).

In the NR pseudo-potential generation, the KS equations were solved self-consistently in the spherically symmetric effective potential for the atom, while in the SR ones, the simplified Dirac's equations, in which the spin-orbit term in the Hamiltonian is initially omitted but the "mass-velocity" and "Darwin" terms were retained [22], were solved self-consistently. Finally, for the FR case, the two-coupled equations (A.4)-(A.5) are solved self-consistently. Even though the valence electrons may have small speeds compared to the inner relativistic electrons, their orbitals also undergo some modifications because the effective potentials were modified via the contributions of high-speed core electrons.

2.2 Electronic structure of UO_2

All calculations are based on the solution of the KS equations in DFT using the Quantum-ESPRESSO code package [23, 24]. Performing convergency tests, the appropriate kinetic energy cutoffs for the plane-wave expansions were chosen as 350 and 1400 Ry for the wave functions and charge densities, respectively. To avoid the self-consistency problems, we have used the Methfessel-Paxton smearing method [25] for the occupations with a width of 0.01 Ry. For the Brillouin-zone integrations in geometry optimizations, a $6\times6\times6$ grid with a shift were used; while for density-of-states (DOS) calculations, we have used a denser grid of $8\times8\times8$ in reciprocal space and "tetrahedron" method [26] for the occupations. In DFT+U calculations, we have chosen the optimum value of 4.0 eV for Hubbard-U, which whenever used in conjunction with non-orthogonalized projection to Hubbard atomic orbitals, reproduces the experimental lattice constant. Taking into account the $Fm\bar{3}m$ constraint, all geometries were fully optimized for total pressures on unit cells to within 0.5 kbar, and forces on atoms to within 10^{-6} Ry/a.u. To handle the multi-minima total energy function for the lowest energy in DFT+U approach, we have used the occupation-matrix control (OMC) method [27] which was also previously used by others [11, 19]. Examining different XC schemes, we found that the generalized gradient approximation (GGA-PBEsol) [28, 29] results in the best agreement with the experimental lattice constant (by construction) and the band-gap. Therefore, in the calculations of this work we employ GGA-PBEsol. Finally, in all our calculations, the simplified model of 1k-order AFM configuration for uranium atoms were used.

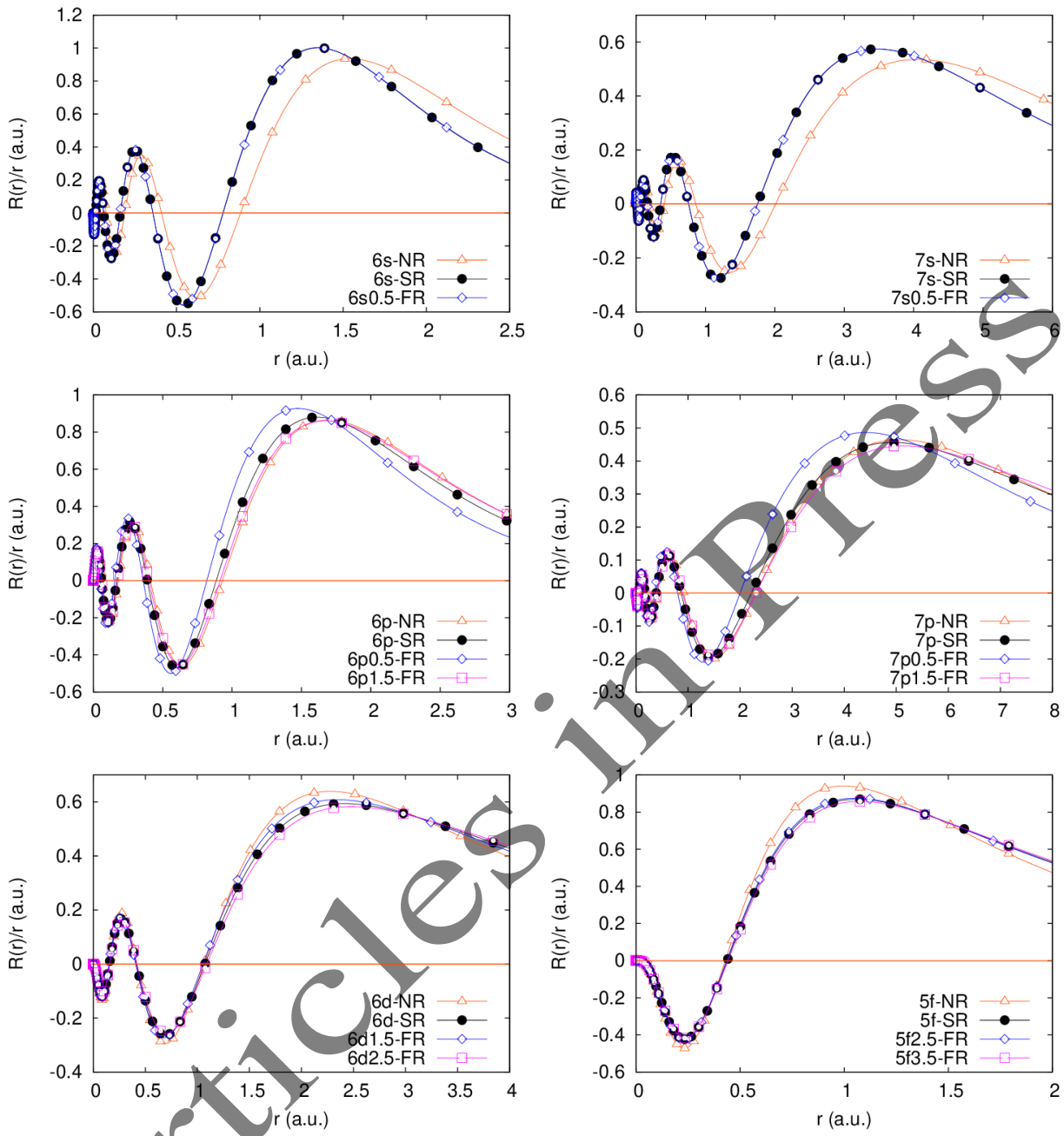

Fig. 2: All-electron U-atomic valence orbitals for NR, SR, and FR cases. As is seen, the *6s* and *7s* orbitals in the NR case are spatially expanded relative to SR and FR cases, and this, in turn, leads to the increase of equilibrium lattice constant in NR level of computations.

3. Results and discussions

3.1 Pseudopotentials

The pseudo-potentials for U and O atoms were generated using the APE code package. In Fig. 2, we have compared the atomic all-electron valence orbitals *6s*, *6p*, *7s*, *7p*, *6d*, and *5f* radial wave-functions for U-atom. As is seen, the *6s* and *7s* orbitals in the NR case are spatially expanded relative to SR and FR cases, and this, in turn, would lead to larger equilibrium lattice constant in NR case. For oxygen, the atomic all-electron valence orbitals *2s*, and *2p* are compared in Fig. 3. As is clearly seen, the relativistic treatment of O-atom does not bring any corrections to the NR orbitals. However, for the sake of consistency we use the same regime for U and O pseudo-potentials in NR, SR, and FR calculations of UO_2.

3.2 Electronic structure of UO_2

As was mentioned in the above, using the GGA-PBEsol approximation for the exchange-correlation leads to excellent agreement with experimental results. To take into account the anti-ferromagnetic configuration of U atoms, we have used a simplified 1k-AFM configuration in which the U atoms change the magnetization in the *z* direction alternatively. The geometries were optimized with the constraint of $Fm\bar{3}m$ space group. In the DFT+U calculations, to avoid meta-stable states, we have used the OMC method.

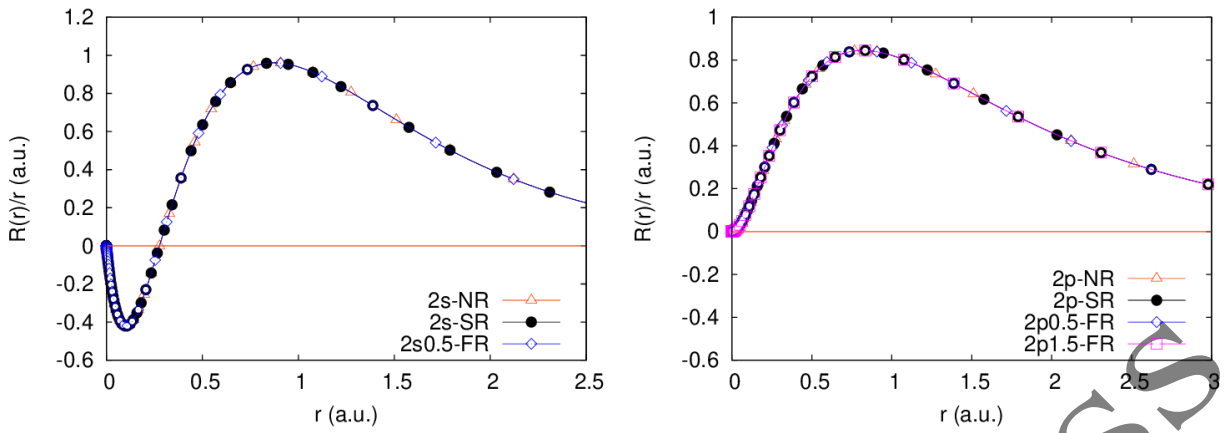

Fig. 3: All-electron O-atomic valence orbitals for NR, SR, and FR cases. As is seen, the *2s* and *2p* orbitals in all cases of NR, SR, and FR are more or less the same.

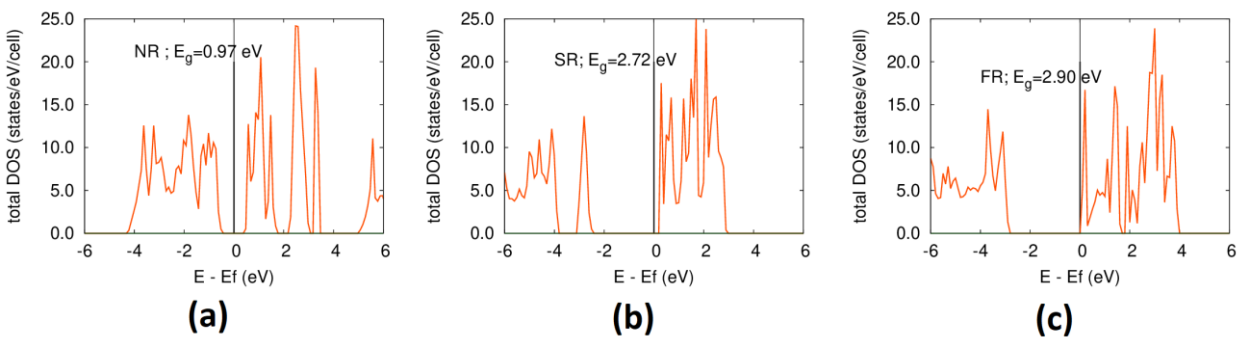

Fig. 4: Electron density of states (DOS) for the NR, SR, and FR cases. The Fermi energies lie inside the gaps, leading to insulator properties for the three cases.

Table 2: Equilibrium lattice constant, *a*, in Angstrom; Kohn-Sham electronic band gap, E_g , in eV for the three schemes of NR, SR, and FR compared with experimental values.

scheme	$a(\AA)$	E_g (eV)
NR	5.588	0.97
SR	5.480	2.72
FR	5.477	2.90
Exp.	5.470	2.20

In Fig. 4, the total electron density of states (DOS) are plotted for the three cases. It is found that the ground states are insulators for all the three cases.

In Table 2, the results for equilibrium lattice constants are listed. As is seen, the difference in the lattice constant is very small in the FR and SR approaches (0.05%) while the electronic gaps differ significantly (by 6.2%). On the other hand, the equilibrium lattice constants in the SR and NR cases differ relatively significantly (by 2%) and the difference in the energy gap is very large (64%). These findings show that the NR scheme for both geometric and electronic properties are very far from experimental values and must be discarded in the study of UO_2. On the other hand, using the SR regime is quite accurate whenever one concerns the geometric properties and not the electronic excitation properties.

In Fig. 4, the total electron density of states (DOS) are plotted for the three cases. It is found that the ground states are insulators for the three cases.

4. Conclusions

In this work, it was shown that the inner electrons of U atom have speeds comparable to that of light and one has to take into account the relativistic effects. However, these effects for the O atom is negligible. NCPP's were generated in three NR, SR, and FR levels and used for the calculation of the properties of UO_2 crystal. The AFM configuration of U atoms were modeled by a simplified 1k-order AFM. In the DFT+U calculations, to avoid meta-stable states, the occupation-matrix control method was used. The results showed that NR scheme predict incorrect results for both geometric and electronic properties and must be avoided. However, the SR and FR approximations give accurate and more or less similar results for the geometric properties (0.05% difference in lattice constant), but the band gaps differ by 6.2% and one would expect differences in the excitation energies.

5. Acknowledgement

This work is part of research program in School of Physics and Accelerators, NSTRI, AEOI.

6. Data availability

The raw or processed data required to reproduce these results can be shared with anybody interested upon sending an email to M. Payami.

7. Appendix A. Dirac Equation

The Dirac equation for an electron in a scalar potential V is given by

$$\hat{H}_D \Psi(\vec{r}) = E\Psi(\vec{r}) \tag{A.1}$$

$$\hat{H}_D \equiv c(\vec{\alpha}\cdot\vec{p}) + \beta mc^2 + VI_4 \tag{A.2}$$

$$\alpha_i = \begin{pmatrix} 0 & \sigma_i \\ \sigma_i & 0 \end{pmatrix} \quad \beta = \begin{pmatrix} I_2 & 0 \\ 0 & I_2 \end{pmatrix} \; ; \; (i = 1,2,3), \tag{A.3}$$

in which σ_i's are Pauli matrices and I_2 is a two-dimensional unit matrix. $\vec{p}$, m, and c are electron momentum, electron rest mass, and light speed in vacuum, respectively.

For a scalar potential with spherical symmetry, it can be shown that the Dirac equation transforms to the following two coupled equations:

$$-\frac{\hbar^2}{2M}\frac{1}{r^2}\frac{d}{dr}\left[r^2\frac{dg_{n\kappa}}{dr}\right] + \left[V + \frac{\hbar^2}{2M}\frac{l(l+1)}{r^2}\right]g_{n\kappa} - \frac{\hbar^2}{4M^2c^2}\frac{dV}{dr}\frac{dg_{n\kappa}}{dr} - \frac{\hbar^2}{4M^2c^2}\frac{dV}{dr}\frac{1+\kappa}{r}g_{n\kappa} = E'g_{n\kappa} \tag{A.4}$$

$$\frac{df_{n\kappa}}{dr} = \frac{1}{\hbar c}(V - E')g_{n\kappa} + \frac{\kappa - 1}{r}f_{n\kappa}. \tag{A.5}$$

Here, we have used

$$\Psi(\vec{r}) = \begin{pmatrix} \psi^1(\vec{r}) \\ \psi^2(\vec{r}) \end{pmatrix} = \begin{pmatrix} g_{nj}(r)\phi_{jlm}(\vartheta,\varphi) \\ if_{nj}(r)\phi_{jlm}(\vartheta,\varphi) \end{pmatrix}, \tag{A.6}$$

where, the spinor-angle functions ϕ_{jlm} are defined as products of spherical harmonics and spinors, and for $j = l \pm 1/2$ are given by:

$$\phi_{jlm} = \left[\frac{(l+1/2)\pm m}{2l+1}\right]^{1/2} Y_l^{m-1/2}\begin{pmatrix}1\\0\end{pmatrix} \pm \left[\frac{(l+1/2)\mp m}{2l+1}\right]^{1/2} Y_l^{m+1/2}\begin{pmatrix}0\\1\end{pmatrix}. \tag{A.7}$$

In the above equations, the following definitions were used:

$$E' = E - mc^2 \; , \; M(r) = m + \frac{E' - V(r)}{2c^2}$$

$$j = l + \frac{\lambda}{2} \; , \; \kappa = -\lambda(j + \frac{1}{2}) \; , \; \lambda = +1, -1 \tag{A.8}$$

$$j = l + \frac{1}{2} \rightarrow \kappa = -(l+1) \; , \; j = l - \frac{1}{2} \rightarrow \kappa = +l.$$

In the left hand side of Eq. (4), the second, third, and fourth terms are the so-called "mass-velocity", "Darwin", and "spin-orbit" terms.

8. References

1. G. Amoretti, et al; Phys. Rev. B 40 (1989) 1856.
2. J. Faber, G. H. Lander, and B. R. Cooper ; Phys. Rev. Lett. 35 (1975) 1770.
3. M. Idiri, T. Le Bihan, S. Heathman, and J. Rebizant; Phys. Rev. B 70 (2004) 014113.
4. L. Y. Desgranges, Ph. Ma, G. Garcia, D. Baldinozzi, H. E. F. Simeone; Inorg. Chem. 56 (2017), 321.
5. Y. Baer and J. Schoenes; Solid State Commun. 33 (1980) 885.
6. J. Schoenes; J. Appl. Phys. 49 (1978) 1463.
7. V. A. Gubanov, A. Rosen, and D. E. Ellis; Solid State Commun. 22 (1977) 219.
8. S. L. Dudarev, et al; Physica status solidi (a) 166 (1998) 429.
9. J. Schoenes; Phys. Rep. 63 (1980) 301.
10. S. L. Dudarev, D. N. Manh, and A. P. Sutton; Phil. Mag. B 75 (1997) 613.
11. B. Dorado, B. Amadon, M. Freyss, and M. Bertolus; Phys. Rev. B 79 (2009) 235125.
12. J. T. Pegg, X. Aparicio-Angles, M. Storr, and N. H. de Leeuw, Nora; J. Nucl. Materials 492 (2017) 269.
13. S. Sheykhi and M. Payami; Physica C: Superconductivity and its Applications 549 (2018) 93.
14. M. S. Christian, E. R. Johnson, and T. M. Besmann; J. Phys. Chem. A 125 (2021) 2791.
15. P. Hohenberg and W. Kohn; Phys. Rev. 136 (1964) B864.
16. W. Kohn and L. J. Sham; Phys. Rev. 140 (1965) A1133.
17. M. Cococcioni and S. de Gironcoli; Phys. Rev. B 71 (2005) 035105.
18. B. Himmetoglu, A. Floris, S. de Gironcoli, and M. Cococcioni; Int. J. Quantum Chem. 114 (2014) 14.
19. M. Freyss, B. Dorado, et. al.; Ψ_k Scientific Highlight of The Month No. 113 (2012).
20. R. A. Evarestov, A. I. Panin, and A. V. Bandura; Russian J. General Chem. 78 (2008) 1823.
21. M. J. T. Oliveira and F. Nogueira; Comput. Phys. Commun. 178 (2008) 524.
22. D. D. Koelling and B. N. Harmon; J. Phys. C: Solid State Physics 10 (1977) 3107.
23. P. Giannozzi, et. al; J. Phys.: Condens. Matter 21 (2009) 395502.
24. P. Giannozzi, et. al.; J. Chem. Phys. 152 (2020) 154105.
25. M. P. Methfessel and A. T. Paxton; Phys. Rev. B 40 (1989) 3616.
26. P. E. Blochl, O. Jepsen, and O. K. Andersen; Phys. Rev. B 49 (1994) 16223.
27. M. Payami; arXiv:2302.04231v1 [cond-mat.mtrl-sci] (2023).
28. J. P. Perdew, A. Ruzsinszky, G. I. Csonka, O. A. Vydrov, G. E. Scuseria, L. A. Constantin, X. Zhou, and K. Burke; Phys. Rev. Lett. 100 (2008) 136406.

29. J. P. Perdew, A. Ruzsinszky, G. I. Csonka, O. A. Vydrov, G. E. Scuseria, L. A. Constantin, X. Zhou, and K. Burke; Phys. Rev. Lett. 102 (2009) 039902.